Performance Characteristics of an Auto-Rotating Lander under High-Speed Deployment

Rais A. Nurhidajat*
Vanderbilt University, Nashville, TN, USA

Auto-rotating landers actively develop aerodynamic lift forces during descent to safely descend and land from altitude. Their simplicity in construction and operation makes them well suited for aerial small payload delivery with applications in ecological monitoring, disaster relief operations, and medical supply distribution in distressed areas. This study presents the design and fabrication of an auto-rotating lander with a mass of 5 lbs. designed to achieve a landing velocity of below 30 ft/s, allowing for landing kinetic energy below 75 lbf-ft. The lander is instrumented with a 6 axis IMU and barometer sensor to allow for a comparison of lander's flight data to an auto-rotation model. The model utilizes Blade Element Theory (BET) to simulate the spin up of lander rotor. The lander was tested under high-speed deployment to validate flight stability and recovery to nominal landing. The lander was successfully able to recover from an initial downwards velocity of up to 70 ft/s. Following successful flight and recovery of the lander testbed, efforts are being directed at developing a biodegradable lander with minimal environmental footprint.

I. Nomenclature

AoA	=	Angle of Attack
AGL	=	Above Ground Level
BET	=	Blade Element Theory
CD	=	Coefficient of Drag
CFD	=	Computational Fluid Dynamics
CG	=	Center of Gravity
CL	=	Coefficient of Lift
COTS	=	Commercial Off the Shelf
CP	=	Center of Pressure
NACA	=	National Advisory Committee for Aeronautics
YPR	=	Yaw, Pitch, and Roll

II. Introduction

AUTO-ROTATION is a state where rotary-winged aircraft's rotor torque and lift are driven by an upward flow of air during descent. This process is useful in auto-rotating landers because it does not require a powerplant, reducing electro-mechanical complexity and mass. Auto-rotating landers provide key benefits over parachutes. They are not impacted by winds as much as parachutes due to a lower projected side area and thereby can have a straighter and more accurate trajectory. Their deployment is also simpler as they do not need a parachute to be carefully packed and either attached to a static line or dropped with an orientation that ensures the package does not fall into the parachute during descent. In contrast, an auto-rotating lander can be designed to drop with any orientation.

There is a plethora of literature analyzing auto-rotation in the context of helicopter flight [1] or decelerators for various applications including planetary probe landings where the atmosphere permits [2]. Most literature discussing decelerators is focused on steady-state auto-rotation [3] and improving modeling methods, mostly in the context of helicopter flight. Literature related to lighter weight auto-rotating decelerators focuses on creating a practical model

---

* Undergraduate Student, Department of Mechanical Engineering, 2301 Vanderbilt Place, Nashville, TN, 37240, AIAA Student Member 1923737, Undergraduate Category.

for a given task [4 - 6]. There is little experimental work on studying auto-rotation under high-speed deployment and irregular orientation, both of which could represent real-world scenarios during deployment. The latter flight data are critical as ideal deployment may not be feasible in an aerial payload delivery context, especially when many payloads are dropped almost simultaneously to complete a mission.

This study will experimentally examine the flight performance of an auto-rotating lander with a mass of 4.4 lbs. and a 4 ft diameter rotor under high-speed deployment. The lander is lifted to an altitude of 600 ft AGL via hexacopter before being released by an electronic latch using ground radio control. Delayed rotor opening was achieved by placing a shroud over the folding rotor blades attached to the duty hexacopter with shock cords of varying length. Experimental data has shown that the auto-rotating lander can return to nominal flight under varying initial velocity and orientation during rotor spin up following shroud release and rotor opening.

III. Lander Design

A. Auto-rotation Modeling and Simulation

A simulation of an auto-rotating lander was scripted in MATLAB to characterize expected landing velocities and loads during flight. Blade element theory (BET) was utilized to calculate the aerodynamic forces across one blade before being quadrupled – for the total number of blades – to calculate the lift, drag, and torque across the entire rotor.

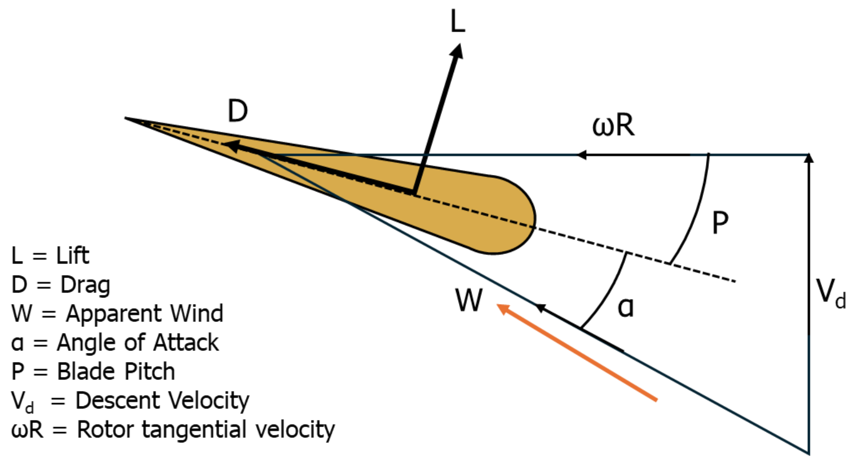

Fig. 1 Blade profile during auto-rotating descent.

The study lander is only simulated in the vertical axis and does not take lander tilt or side winds into account. The blades have a NACA 0012 symmetrical profile and the CD and CL of the profile at various angles of attack (AoA) were taken from NACA Technical Note 3361 [6]. The blades on the lander can flap up and down via blade grips, however the blade flapping is not modeled in the simulation. Also, the blades are fixed within the plane of rotation in the simulation, and rotor opening is not modeled.

The lander's flight is simulated using explicit Euler integration starting at a given height and concluding once the lander strikes the ground. The body of the lander is given a representative diameter of 6 in and a CFD determined CD of 0.5. This drag force is combined with the thrust of the rotor to simulate the lander performance more accurately.

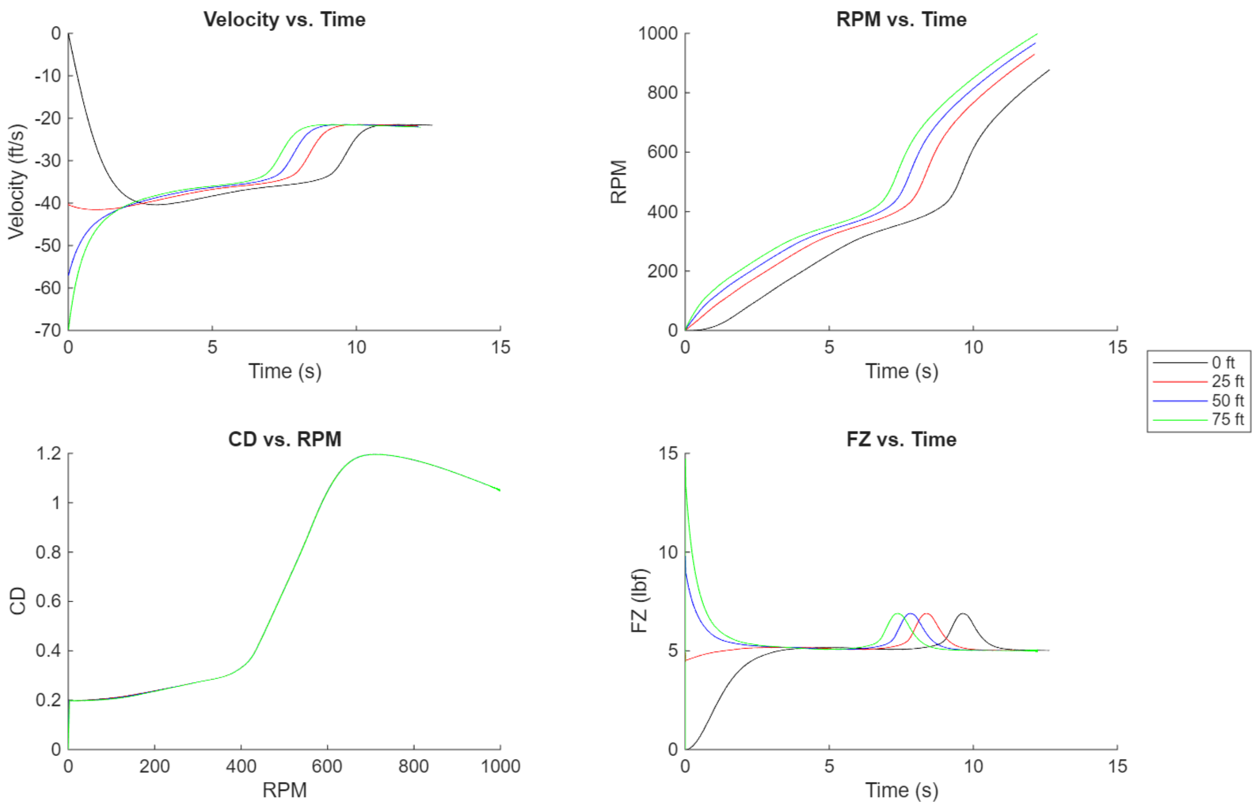

Fig. 2 Simulated flight data for varying free-fall distances. Lander is given varying initial velocity to simulate the free-fall portion of flight. CD is with respect to rotor area, and FZ is total upwards force acting on the lander.

The simulation is most valid for steady-state auto-rotation. Transient spin up is inherently chaotic due to AoA approaching 90 degrees when the rotor speed is low. During flight, the lander may also fall sideways which further increases the time for rotor spin up and complicates modeling the transient portion of flight.

The values of most interest from these simulations are the landing velocity and peak rotor force as those drive design constraints for the lander and safety of the payload. The lander was designed to have a landing kinetic energy below 75 lbf-ft. Given the 4.4 lb. lander mass, this yields a landing velocity of under 33.1 ft/s. The simulations yield a landing velocity around 20 ft/s for all flights with a variation of 0.5 ft/s.

B. Lander Construction

The lander uses COTS carbon fiber blades with a chord of 2 in and length of 24 in produced by *XLPower Heli*. These blades are symmetrical in profile with a NACA 0012 airfoil and are not twisted. The blades are attached to aluminum grips which are attached to the rotor head at a fixed -5-degree angle with a bolt. The blade grips allow the blades to flap up or down and allow the lander to stabilize beneath the rotor more easily. The rotor head sits on a ball bearing to minimize friction as the rotor spins up. The rotor head is attached to an aluminum rod that runs down the central axis of the lander attaching to the nosecone and flight computer by an aluminum bulk plate. The current lander design has a weight of 4.4 lbs., with 3.1 lbs. allocated to the rotor head and shaft and 1.3 lbs. to the electronics and nosecone.

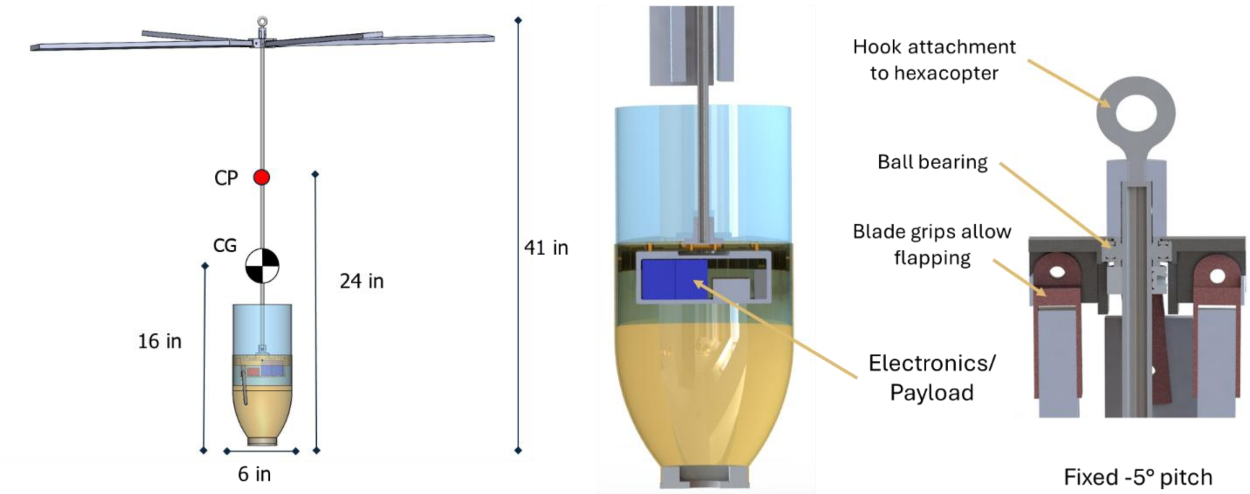

Fig. 3 Lander design

Fig. 4 Completed lander construction

The lander was designed to be statically stable with a lower CG compared to CP. CP was estimated by using *COMSOL* CFD modeling with the assumption that the rotor acted as a solid disc. This design is inherently more stable with a greater payload mass as the CP is only affected by external geometry.

C. Lander Instrumentation

The lander is instrumented with a *SpeedyBee F405* Wing flight controller commonly utilized in hobby radio-controlled aircraft. This controller has an ICM-42688-P 6 axis IMU (accelerometer and gyroscope) that samples at 25 Hz and a SPL06-001 altimeter that samples at 10 Hz.

IV. Flight Studies

The lander was tested by dropping it from a hexacopter drone. When the drone reached the desired altitude, the rotary latch holding the lander would open from ground RF command, allowing the lander to fall. Once the shock cord extends to full length, the shroud detaches from the rotor and allows it to spin up.

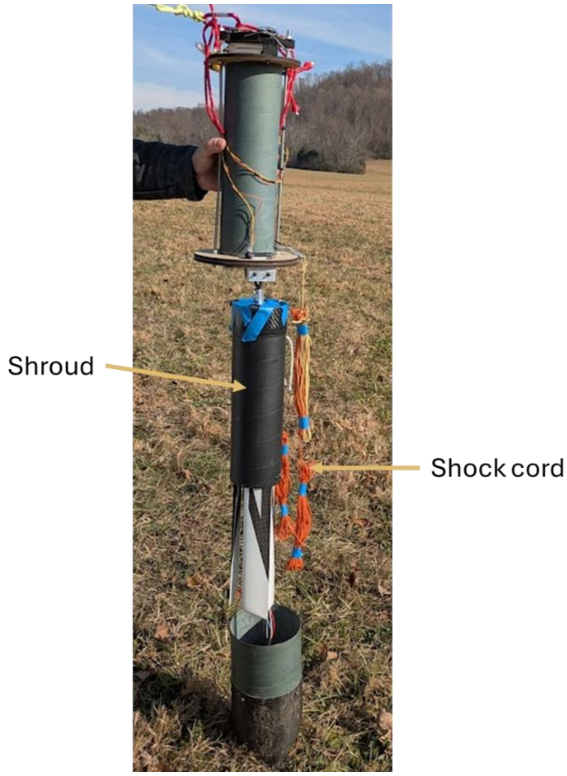

Fig. 5 Lander setup during flight preparation.

A GoPro Hero 12 camera filming at 1080p and 30 Hz was attached to the duty hexacopter facing directly downwards to allow for trajectory analysis of the lander during descent. *Kinovea* – a video annotation tool used in sports analysis – was utilized to automatically track the horizontal and vertical movement of the lander through the frame. This analysis was then time-matched to the altimeter data to create a 3D flight reconstruction.

Fig. 6 In-flight drop test showing descent right after release (left), descent with shroud attached (center), descent just prior to rotor opening following shroud detachment (right).

During descent with shroud attached, the lander is in free-fall, thus the orientation at shroud detachment is unpredictable. The violent action of shroud detachment causes the lander to further tilt into an extreme orientation, nearing 90 deg before the rotor spins up and stabilizes the lander. This non-deterministic nature of shroud detachment also simulates the effect of strong winds and gusts during deployment that could impact lander flight.

V. Results

For field testing, a 0, 50, and 75 ft free-fall deployment and trajectory were examined to test the lander's ability to stabilize. To ensure that the rotor would have ample time to spin up, the drop altitude was set to 600 ft AGL. The side wind on this test day was minimal, with gusts up to 1-2 mph observed.

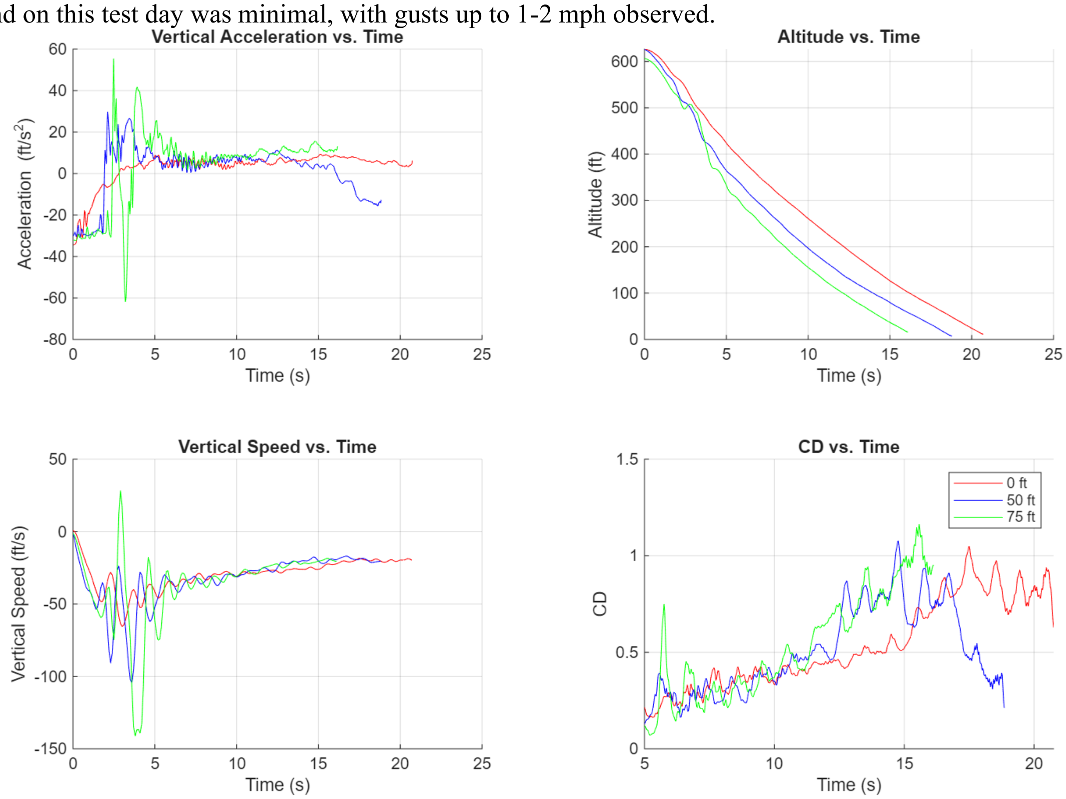

Fig. 7 Flight data from field tests.

All flights stabilized at a nominal descent velocity of around 20 ft/s, confirming the ability of the lander to return to nominal flight under high-speed deployment. There is a slight increase in speed for the 50 ft flight which matches a drop in the acceleration plot on the top left. It is important to note that the vertical acceleration from the IMU is along the vertical axis of the lander, and not a transformation of all 3 acceleration axes. It was observed that the lander began to corkscrew slightly due to gusts of wind which changed throughout the day. This movement caused the lander to tilt in orientation during steady descent, leading to an increase in downwards acceleration in the vertical axis while maintaining the same vertical speed.

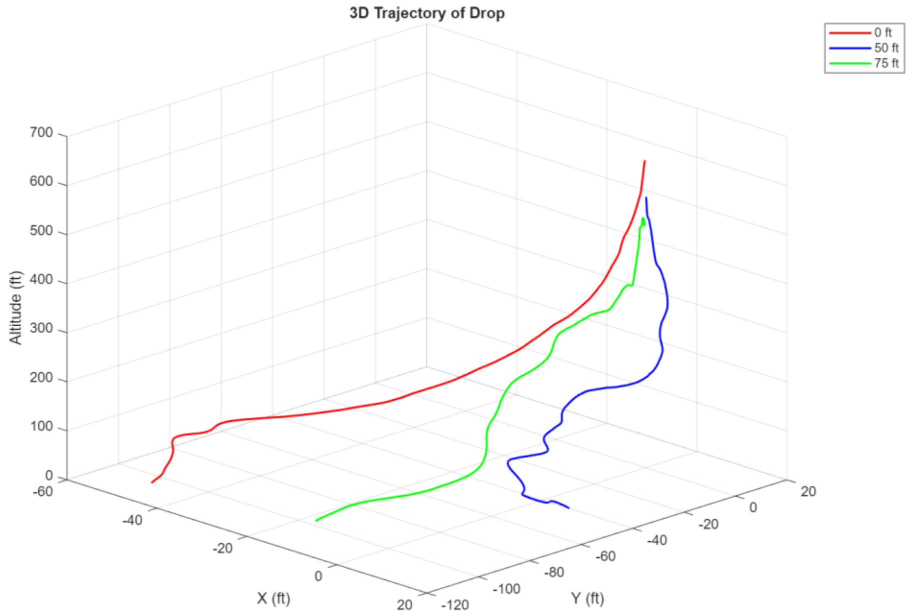

Fig. 8 Trajectory of field tests. Origin centered at shroud opening. Total drift in ft was 112, 42, and 104 for the 0, 50 ft and 75 ft free-fall, respectively.

Figure 9 was generated using the footage from the onboard camera of the duty hexacopter. Using *Kinovea*, the position of the lander was tracked in the x and y directions within the frame and correlated to the measured distance on the ground to find the x and y drift in ft. This footage was time-matched to the altimeter data to generate a 3D plot of the flight from shroud opening.

It can be expected that a higher deployment speed will yield a lower drift. This is because the overall flight is shorter and for a given wind it should drift less. However, as can be seen in the figure above, the 50 ft flight has the lowest drift while the 75 ft flight drifted nearly to the same spot as the 0 ft flight. Inherently, the unpredictable but stabilizing nature of transient rotor spin up following shroud release means that the lander turns to very extreme angles. Thus, as the rotor spins up and generates lift it will pull the lander sideways. Small changes in wind can also change the overall direction of drift, as was the case during these tests. The extreme angles in orientation that the lander experiences during transient rotor spin up can be seen very clearly in the following figure (Figure 9):

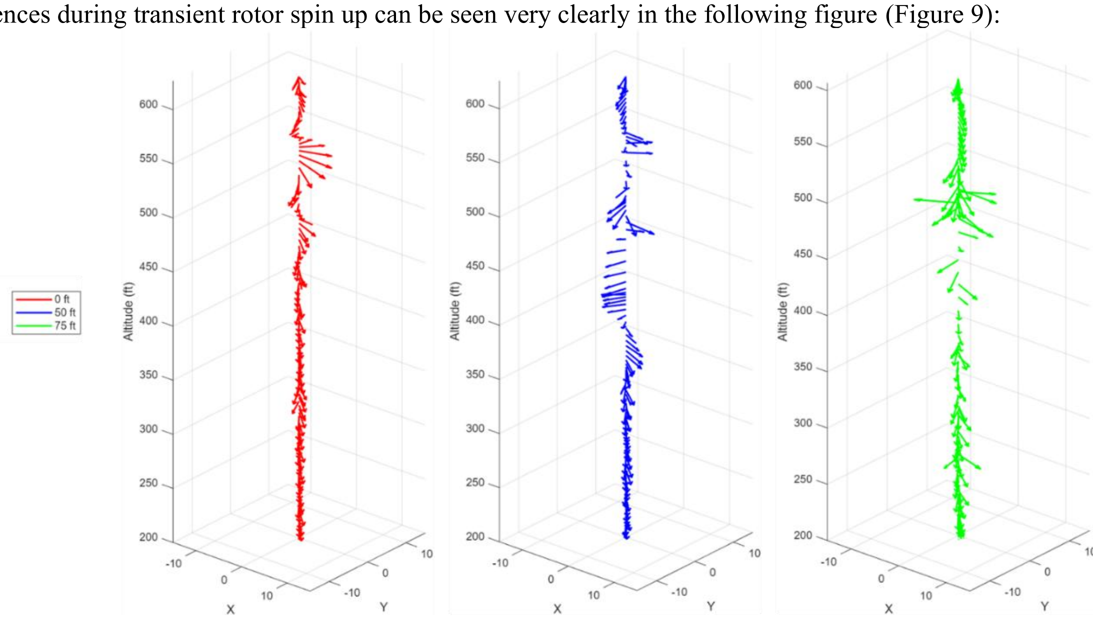

Fig. 9 Orientation data for Round 2 tests

Figure 9 shows the chaotic nature of transient rotor spin up during the first few hundred feet of descent. For example, the point where the shroud detaches from the lander in the 75 ft flight is extremely clear where the direction of the vectors drastically changes following the initial 75 ft of descent. All three flights show an initial sideways free-fall following rotor opening. This effect is most visible in the 50 ft flight as the lander's rotor took nearly 200 ft to fully spin up.

This figure (Figure 9) was generated using the onboard gyroscope to plot vectors with the arrows pointing down away from the rotor. The Euler angles of YPR, and angular velocities were taken to find the orientation of the lander. During descent, the lander experienced a body yaw due to the torque of the rotor. This fact combined with the fact that the lander did not fly perfectly level led to significant noise in the YPR. To counteract this, the vectors were weighted with a transformation of the angular velocities. The angular velocity around the shaft (yaw) is much higher than that around the roll and pitch axes. This weighting allows for a more accurate representation of the lander orientation as it descended. The origin of the vectors was found by time-matching the gyroscope data to the altimeter data.

Table 1 Flight stability data

Drop altitude/ Freefall distance (ft)	Rotor spin up time (s)	Change in altitude during rotor spin up (ft)
600/0	3.0	90
600/50	2.2	130
600/75	3.2	190

As can be seen in Table 1, rotor spin up varies considerably in time even with the same initial vertical speed. This is to be expected due to the initial conditions at deployment coupling with rotor deployment. The change in altitude during rotor spin up provides a floor for the deployment altitude at various vertical speeds. The auto-rotating lander requires a minimum of 100 ft AGL of altitude prior to deployment which grows to a minimum of 200 ft AGL for a vertical velocity of 70 ft/s (free-fall distance of 75 ft).

Table 2 In-flight forces and landing speeds. Landing speed was simulated to be ~20 ft/s for all flights.

Drop altitude/ Freefall distance (ft)	Landing Speed (ft/s)	Peak Rotor Force (lbf)	Simulated Peak Rotor Force (lbf)
600/0	20.7	5.7	6.9
600/50	20.8	8.4	9.8
600/75	20.7	12.0	14.7

The peak rotor force was taken to be the vertical axis of the accelerometer (Table 2). As mentioned earlier, the simulation does not simulate the free-fall itself, just given an initial velocity with the rotor already completely open.

VI. Conclusion

An autorotating lander was successfully able to recover from a high-speed deployment of up to 70 ft/s (free-fall distance of 75 ft), with the rotor taking up to 3.2 s to spin up. This confirms expectations from static analysis where a low CG will allow for the lander to right itself regardless of initial orientation or speed. The lander requires a minimum of 100 to 200 ft altitude AGL to completely stabilize prior to landing and can be dropped from higher altitudes without any negative effect on stability. These altitudes are well within the operating constraints of most aircraft – to include manned and unmanned aircraft – capable of lifting 5 lb. payloads.

The observed rotor forces demonstrate that for the given flights, the current lander design using aluminum and carbon fiber could be re-designed to use more lightweight and inexpensive materials. Most applications would necessitate the use of materials that are biodegradable. In future work, instrumentation of rotor blades will inform the fabrication of rotor blades and lander structures using biodegradable materials that will minimize environmental impact and reduce construction cost. Also, there will not be any need for electronics or instrumentation while dropping needed supplies.

This work has proven that an autorotating lander can right itself under high-speed deployment (equivalent to delayed rotor opening), and varying release orientations. These tests also add to the expectation that moderate side winds will not jeopardize the lander's ability to land safely, as it can stabilize in flight. The flight stability of the lander can also be further evaluated by conducting flight testing during conditions of higher side winds and gusts or dropping the lander from a moving aircraft.

VII. Appendix

1) XLPower Heli Hawk 600mm Carbon Fiber Blades: (https://www.helidirect.com/products/hawk-600mm-carbon-fiber-blades)
2) COMSOL: (https://www.comsol.com/comsol-multiphysics)
3) Go Pro Hero 12 Camera: (https://gopro.com/en/as/shop/cameras/hero12-black/CHDHX-121-master.html)
4) SpeedyBee F405 Wing Controller: (https://www.speedybee.com/speedybee-f405-wing-app-fixed-wing-flight-controller/)
5) Kinovea: (https://www.kinovea.org/)

VIII. Acknowledgments

The author would like to thank Vanderbilt Aerospace Design Laboratory undergraduate independent study contributors for their assistance in various phases of this study. The research conducted at VADL was supported by the Mark Dalton Fund for Experiential Learning in Aerospace Engineering.

References

[1] Nikolsky, A. A., Seckel, E., "An Analytical Study Of The Steady Vertical Descent In Autorotation Of Single-Rotor Helicopters," NACA TN 1906, 1949

[2] Young, L. A., Briggs, G., Aiken, E., Pisanich, G., "Rotary-Wing Decelerators for Probe Descent Through the Atmosphere of Venus," *2nd International Planetary Probe Workshop*, 2005

[3] Houston S.S., Brown, R. E., "Rotor-Wake Modeling for Simulation of Helicopter Flight Mechanics in Autorotation", *Journal of Aircraft*, Vol. 40 No. 5, 2003

[4] Mitchell, J., Marshall J. A., "Design Of A Novel Auto-Rotating UAV Platform For Underground Mine Cavity Surveying", Master's Thesis, Queen's University, Ontario, CA, 2017

[5] Jain, P., Sirohi, J., Cameron, C., "Design, Analysis, and Testing of a Passively Deployable Autorotative Decelerator," *Journal of Aircraft*, Vol. 59, No. 1, 2022

[6] Critzos, C. C., Heyson, H. H., Boswinkle Jr., R. W., "Aerodynamic Characteristics Of NACA 0012 Airfoil Section At Angles of Attack From 0˚ To 180˚," NACA TN 3361, 1955